


RESEARCH

Open Access



Protective role of small extracellular vesicles derived from HUVECs treated with AGEs in diabetic vascular calcification

Bei Guo¹, Su-Kang Shan¹, Feng Xu¹, Xiao Lin², Fu-Xing-zi Li¹, Yi Wang¹, Qiu-Shuang Xu¹, Ming-Hui Zheng¹, Li-Min Lei¹, Chang-Chun Li¹, Zhi-Ang Zhou⁴, Muhammad Hasnain Ehsan Ullah¹, Feng Wu³, Xiao-Bo Liao⁴ and Ling-Qing Yuan^{1*} 

Abstract

The pathogenesis of vascular calcification in diabetic patients remains elusive. As an effective information transmitter, small extracellular vesicles (sEVs) carry abundant microRNAs (miRNAs) that regulate the physiological and pathological states of recipient cells. In the present study, significant up-regulation of miR-126-5p was observed in sEVs isolated from human umbilical vein endothelial cells (HUVECs) stimulated with advanced glycation end-products (A-EC/sEVs). Intriguingly, these sEVs suppressed the osteogenic differentiation of vascular smooth muscle cells (VSMCs) by targeting BMPR1B, which encodes the receptor for BMP, thereby blocking the smad1/5/9 signalling pathway. In addition, knocking down miR-126-5p in HUVECs significantly diminished the anti-calcification effect of A-EC/sEVs in a mouse model of type 2 diabetes. Overall, miR-126-5p is highly enriched in sEVs derived from AGEs stimulated HUVECs and can target BMPR1B to negatively regulate the trans-differentiation of VSMCs both in vitro and in vivo.

Keywords: Vascular calcification, Diabetes, sEVs, miR-126-5p, Endothelial cells

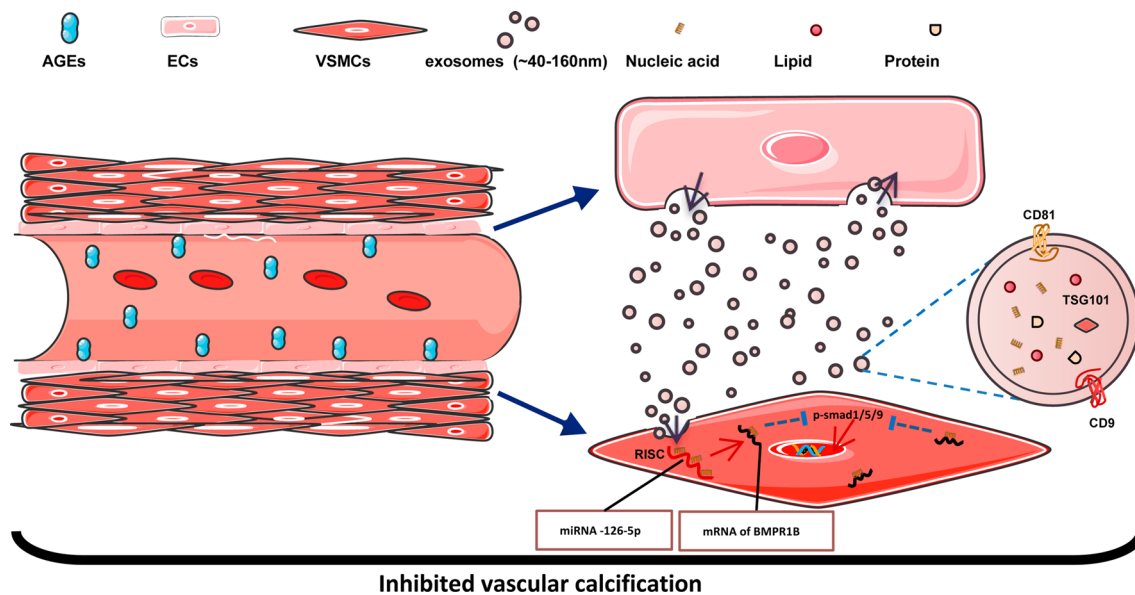
*Correspondence: allenylq@csu.edu.cn

¹ National Clinical Research Center for Metabolic Diseases, Department of Metabolism and Endocrinology, The Second Xiangya Hospital, Central South University, Changsha 410000, China
Full list of author information is available at the end of the article



© The Author(s) 2022. **Open Access** This article is licensed under a Creative Commons Attribution 4.0 International License, which permits use, sharing, adaptation, distribution and reproduction in any medium or format, as long as you give appropriate credit to the original author(s) and the source, provide a link to the Creative Commons licence, and indicate if changes were made. The images or other third party material in this article are included in the article's Creative Commons licence, unless indicated otherwise in a credit line to the material. If material is not included in the article's Creative Commons licence and your intended use is not permitted by statutory regulation or exceeds the permitted use, you will need to obtain permission directly from the copyright holder. To view a copy of this licence, visit <http://creativecommons.org/licenses/by/4.0/>. The Creative Commons Public Domain Dedication waiver (<http://creativecommons.org/publicdomain/zero/1.0/>) applies to the data made available in this article, unless otherwise stated in a credit line to the data.

Graphical Abstract



Introduction

The global incidence of diabetes mellitus (DM) is increasing and diabetic vascular complications are frequent and refractory, leading to high medical and healthcare expenditure [1, 2]. Patients with DM may exhibit extensive vascular media calcification (VC) with disturbed vessel wall homeostasis, characterised by endothelial dysfunction and phenotypic switching of VSMCs, which plays an essential role in the process of VC [3, 4]. However, the pathogenesis of VC in DM is complex and elusive, requiring further exploration.

Small extracellular vesicles (sEVs), diameter < 200 nm, are composed of a lipid bilayer and enclose various types of cargo [5]. sEVs are natural carriers that express CD47, a well-known “don’t eat me” molecule [6, 7]; by expressing this marker, sEVs will not be endocytosed by circulating monocytes. Recently, sEVs have been recognised as novel mediators of intercellular communication [8–10]. sEVs are internalised by various types of cells [11] and deliver their cargo (e.g., proteins, mRNAs and miRNAs) into the cytosol [12], which modifies the physiological or pathological state of recipient cells [13–15]. For instance, mesenchymal stromal cells (MSCs) derived small EVs are rich in miR-126, miR-145 and vascular endothelial growth factors, which effectively inhibit the calcification of synthetic vascular grafts [16]. Therefore, the functional regulation of recipient cells mediated by EVs has great importance in different diseases including VC.

Endothelial cells (ECs) not only form blood vessels to transport nutrients to tissues and remove metabolites, but also secrete bioactive molecules to regulate cell function [17–19]. Once disturbed, ECs secrete a range of self-repairing substances carried by EVs [20–22]. Previous studies have demonstrated that activated or apoptotic ECs produce microparticles that transfer proteins and miRNAs to target ECs, which protect ECs against apoptosis and promote EC repair [21, 23]. VSMCs are located in close proximity to ECs; however, it remains unclear whether sEVs from activated or apoptotic ECs affect vascular calcification.

Advanced glycation end-products (AGEs), generated through a non-enzymatic reaction between sugar residues and proteins or lipids [24], are increased in patients with DM and are correlated with diabetic vascular complications [25, 26]. AGEs activate ECs by binding to RAGE, the receptor for AGEs, which then induces the generation of reactive oxygen species [27], impairing ECs and eventually leading to EC apoptosis [25, 26]. In this study, we sought to investigate whether sEVs released from AGEs stimulated ECs influence vascular calcification.

In the present study, we found that the sEVs secreted by AGEs stimulated human umbilical vein endothelial cells (HUVECs) were rich in miRNA-126 and these sEVs were internalised by VSMCs *in vitro* and *in vivo*. Additionally, the absorbed exosomal miRNA-126 led to the reduced expression of a key osteogenic protein and

calcium deposition by blocking the smad1/5/9 signaling pathway.

Materials and methods

Reagents

Antibodies against RUNX2 (ab23981; Abcam, UK), BMP2 (ab214821; Abcam, UK), BMPR1B (ab175385; Abcam, UK), CD81 (ab79559; Abcam, UK), CD9 (ab92726; Abcam, UK), TSG101 (ab125011; Abcam, UK), p-smad1/5/9 (#13820T; CST, USA), BSA (66201-1; Proteintech, China), PNCA (10205-2-AP; Proteintech, China) and β -actin (20536-1-AP; Proteintech, China) were used in this research. Goat anti-rabbit IgG H&L (Alexa Fluor 488; ab150077) was purchased from Abcam (UK). Horseradish peroxidase (HRP)-conjugated goat anti-mouse secondary antibody and HRP-conjugated goat anti-rabbit secondary antibody were purchased from Santa Cruz Biotechnology (TX, USA). Cy3-conjugated goat anti-rabbit IgG (GB21303) and Alexa Fluor[®]488-conjugated goat anti-mouse IgG (GB25301) were purchased from Servicebio (Wuhan, China). The ECL detection kit (Immobilon[™] Western, WBKLS0100) was purchased from Millipore (MA, USA). The MiRNeasy Serum/Plasma Kit was purchased from QIAGEN (catalogue no. 1071073; ThermoFisher Scientific Inc., USA). Maxima SYBR Green/ROX qPCR Master Mix (C0210B) and primers were purchased from GeneCopoeia (Rockville, MD, USA). MiR-126-5p mimics (miR10000444), inhibitors (miR20000444) and their control oligos were purchased from RiboBio (Guangzhou, China). DAPI (C0065) was purchased from Solarbia (Beijing, China). DMEM/F12 (01-172-1A) and foetal bovine serum (FBS; 04-002-1A) were purchased from Biological Industries (Bioind, Israel). SiRNA-mate (190,903) was purchased from Gene Pharma (Shanghai, China). AGEs (2221-10) were purchased from BioVision (San Francisco, USA). Streptozotocin (STZ, V900890), β -glycerophosphate (β -GP, 50020) and PKH26 Red Fluorescent Cell Linker Kit (PKH26PCL) were purchased from Sigma-Aldrich (St Louis, MO, USA). GW4869 (Umibio, Shanghai, China), DiR (2024243; ThermoFisher Scientific/Invitrogen, Waltham, USA), Alkaline Phosphatase (ALP) Stain Kit (40749ES60; Yeasen, Shanghai, China), Alizarin Red staining (ARS) Kit (G1038; Servicebio, Wuhan, China), ALP assay kit (Nanjing Jiancheng Biotechnology Co., Ltd., China), CCK8 assay kit (SA613; Dojindo, Japan) and NE-PER Nuclear and Cytoplasmic Extraction Reagents (78833; Thermo Scientific, USA) were used in the study.

Isolation and identification of sEVs

HUVECs were cultured in DMEM/F12 (1:1) medium containing 10% exosome-depleted FBS, before being

treated with 100 μ g/mL AGEs for 48 h. Briefly, when the cell confluence was about 30–50%, HUVECs were treated with AGEs and then conditioned media was collected when the confluence reached 90–100%. sEVs were purified from the collected conditioned media according to the published protocol [28]. The HUVEC-derived sEVs were identified by transmission electron microscopy and then submitted to nanoparticle tracking analysis and western blot analysis for the sEVs marker.

RNase treatment

sEVs were treated with or without 1% Triton X-100 and incubated with or without RNase before RNA extraction as previously reported [29].

Statistical analyses

All data are presented as the mean \pm SD of three independent experiments. Data were analysed and plotted using GraphPad Prism software (San Diego, CA, USA) and Image J software (National Institutes of Health). Statistical significance was determined by the unpaired two-sided Student's *t*-test or one-way analysis of variance with LSD or Bonferroni correction for multiple comparisons. A *P*-value < 0.05 was considered statistically significant.

Results

Advanced glycation end-products reduce the viability of HUVECs in a dose and time-dependent manner

To investigate the effects of AGEs on endothelial cells, HUVECs were treated with different concentrations of AGEs (0–400 μ g/mL). The viability of HUVECs was reduced by treatment with 400 μ g/mL AGEs for 48 and 72 h or 200 μ g/mL AGEs for 72 h (Additional file 1: Fig. S1). However, treatment with AGEs at concentrations of 100 and 200 μ g/mL for 48 h did not affect the activity of the HUVECs (Additional file 1: Fig. S1). Therefore, 100 μ g/mL AGEs and 48 h incubation were applied to HUVECs in the following experiments.

Identification of sEVs

sEVs derived from HUVECs stimulated with or without AGEs (EC/sEVs and A-EC/sEVs) were purified from conditioned media. Transmission electron microscopy and nanoparticle tracking analysis demonstrated the lipid-bilayer structure specific of round-shaped EVs with a diameter of 30–200 nm (Fig. 1A, B). These sEVs carried the characteristic exosomal markers CD9, CD81 and TSG101 (Fig. 1C). To determine the topology of EV-associated components, sEVs were treated by proteinase K (PK, a enzyme to degrade only surface exposed components) or Triton X-100 (a detergent capable of penetrating membrane structure). PK digested the plasma transmembrane protein CD9 and CD81, but did not

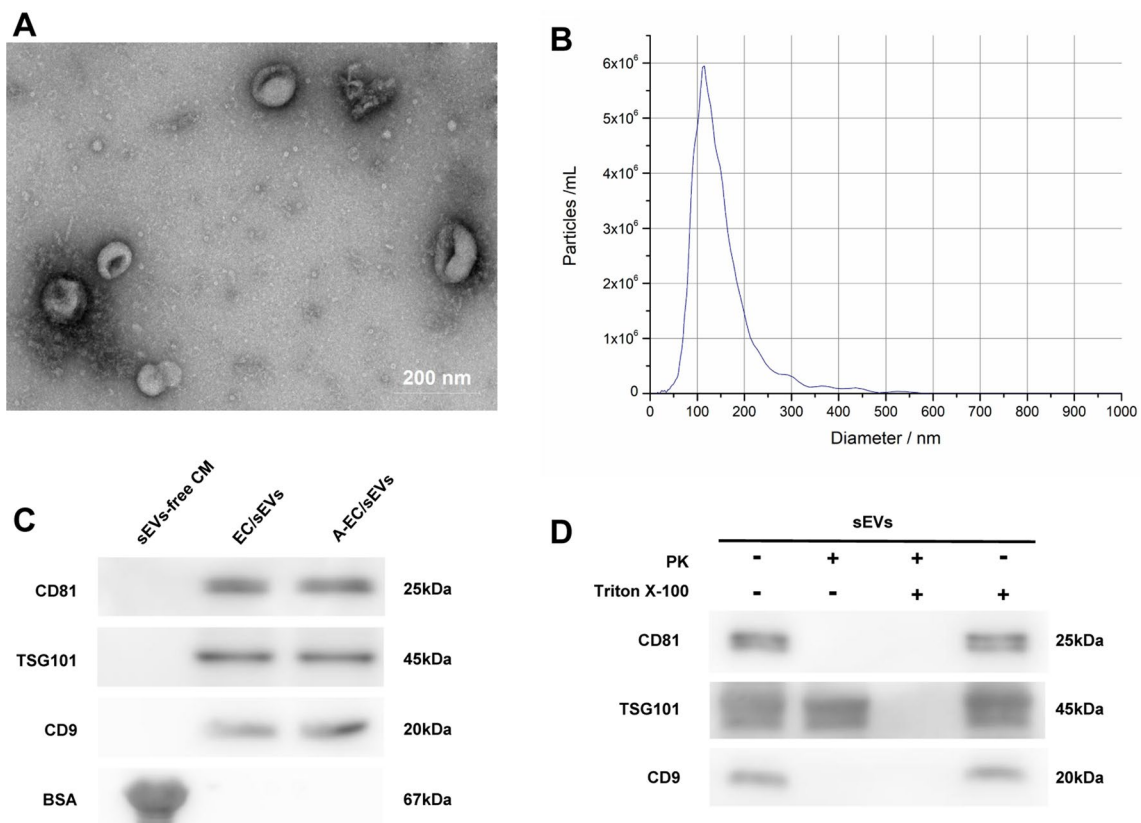


Fig. 1 Identification of EC/sEVs. Small extracellular vesicles (sEVs) derived from HUVECs with or without AGEs pre-treatment (A-EC/sEVs, EC/sEVs). **A** Representative image of the ultrastructure of sEVs observed by transmission electron microscopy. **B** The average particle size distribution of sEVs using nanoparticle tracking analysis. **C** Analysis of the possible contaminants BSA and the sEVs markers CD9, CD81 and TSG101 by western blotting in sEVs preparations. The conditioned media after sEV removal was used as a control. **D** The expression of sEVs markers after proteinase K (PK) or Triton X-100 treatment detected by western blotting

digest the luminal protein TSG 101 (Fig. 1D). In general, the above results confirmed that sEVs were successfully isolated from HUVECs.

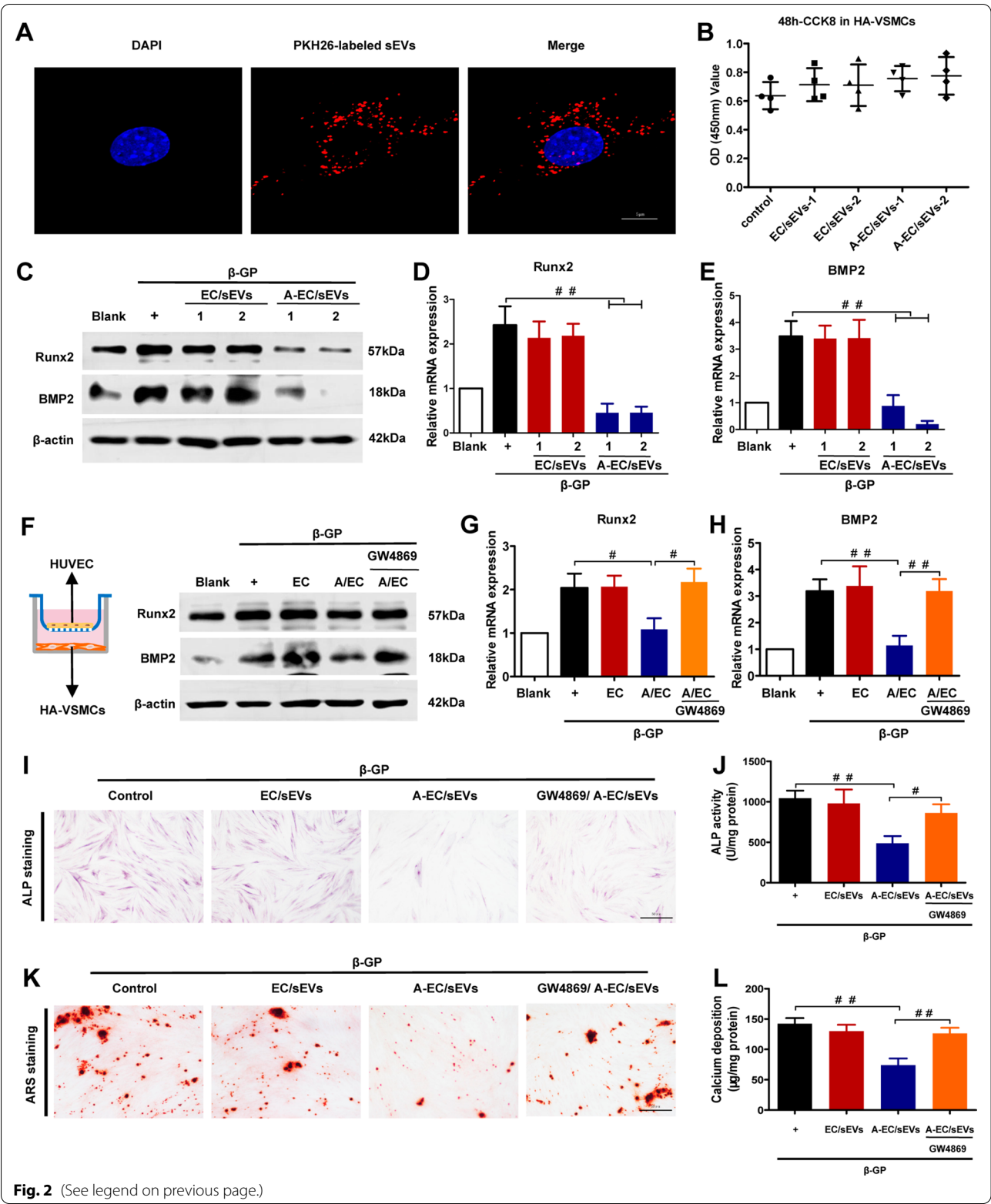
A-EC/sEVs inhibit the calcification of HA-VSMCs in vitro

To explore the roles of A-EC/sEVs on VSMC calcification, we firstly identified human thoracic aortic

vascular smooth muscle cells (HA-VSMCs) by detecting the α -SMA marker (green fluorescence) (Additional file 1: Fig. S2). Then, PKH-26-labelled sEVs secreted from HUVECs were co-incubated with HA-VSMCs for 12 h and the data showed that PKH-26-labelled sEVs (red fluorescence) were efficiently internalised by HA-VSMCs, as evidenced by red

(See figure on next page.)

Fig. 2 A-EC/sEVs inhibited the osteogenic differentiation of HA-VSMCs in vitro. **A** Representative fluorescence micrograph of PKH-26-labelled sEVs (red) internalised by primary HA-VSMCs, while blue represents the nucleus. The labelled sEVs were co-incubated with HA-VSMCs for 12 h. **B** Effect of A-EC/sEVs on the viability of HA-VSMCs (sEVs-1 and sEVs-2 indicate 50 and 100 μ g/mL of sEVs, respectively). CCK-8 values were measured at 48 h post co-incubation. **C** Representative western blot image showing the effect of A-EC/sEVs on the protein levels of Runx2 and BMP2 in β -GP-induced HA-VSMCs after 48 h co-incubation. **D, E** The mRNA levels of Runx2 and BMP2 in HA-VSMCs as measured by qPCR. $^{##}P < 0.01$; data are presented as the mean \pm SD of three replicates. **F** Representative images showing the transwell co-incubation assay of HA-VSMCs and HUVECs pre-treated with or without AGEs or GW4869, respectively, for 48 h. The protein levels of Runx2 and BMP2 in HA-VSMCs. **G, H** The mRNA levels of Runx2 and BMP2 in HA-VSMCs. $^{##}P < 0.01$, $^{*}P < 0.05$; data are presented as the mean \pm SD of three replicates. Alkaline phosphatase (ALP) staining (**I**) and ALP activity (**J**) of calcified HA-VSMCs treated with A-EC/sEVs, EC/sEVs or sEVs from HUVECs pre-treated with GW4869 before AGEs treatment (GW4869/A-EC/sEVs) for 7 days. Alizarin Red staining (ARS) (**K**) and calcium content (**L**) of calcified HA-VSMCs treated with A-EC/sEVs, EC/sEVs or GW4869/A-EC/sEVs for 21 days. Representative micrographs are shown, scale bar represents 50 μ m. $^{##}P < 0.01$, $^{*}P < 0.05$



fluorescence in the cytoplasm and surrounding the nuclei (blue fluorescence stained by DAPI) (Fig. 2A). We next sought to assess whether A-EC/sEVs affect the viability of HA-VSMCs. Different concentrations of EC/sEVs or A-EC/sEVs (ex1 and ex2 indicate 50 and 100 $\mu\text{g}/\text{mL}$ sEVs concentrations, respectively) were added to the HA-VSMCs medium for 48 h. The CCK-8 assay showed that neither EC/sEVs nor A-EC/sEVs affected HA-VSMC viability (Fig. 2B). Lastly, to test whether these sEVs impact on the transformation of VSMCs into osteogenic phenotype, we co-incubated β -glycerophosphate (β -GP)-induced HA-VSMCs (calcified cell model) with different concentrations of EC/sEVs or A-EC/sEVs. Intriguingly, we found that A-EC/sEVs significantly alleviated the increased BMP-2 and Runx2 (markers of osteogenic differentiation) expression compared to the EC/sEVs group (Fig. 2C–E). Furthermore, we constructed a co-culture system of HUVECs and HA-VSMCs through the transwell plate. In this system, β -GP-induced HA-VSMCs in the lower chamber were co-cultured with HUVECs in the upper chamber pre-treated with or without AGEs or GW4869 (an inhibitor to block sEVs production) [30]. As shown in Fig. 2F–H, compared with VSMCs which were co-cultured with HUVECs, the RNA and protein levels of Runx2 and BMP2 in HA-VSMCs which were co-cultured with AGEs pre-treated HUVECs were significantly reduced, but this effect was abolished by GW4869 pre-treatment. To eliminate the role of other soluble molecules, conditioned media with vesicle removed (EC/sEVs-free CM and A-EC/sEVs-free CM) were also employed for the following experiments. Compared to the A-EC/sEVs treatment, A-EC/sEVs-free CM treatment no longer has the effect of down-regulating the expression of Runx2 and BMP2 (Additional file 1: Fig. S3). Together, the data reveal that AGEs stimulated HUVECs reduce the osteogenic differentiation of target cell VSMCs through secreting sEVs rather than soluble mediators. Next, we measured the direct effects of A-EC/sEVs on the activity

of ALP (an early marker of osteogenesis) and calcium deposition (a late marker of osteogenesis) [31]. A-EC/sEVs treatment significantly reduced ALP activity in β -GP-induced HA-VSMCs, but GW4869 pre-treatment in HUVECs significantly abolished the protective effect (Fig. 2I and J). Consistently, A-EC/sEVs treatment strongly alleviated the mineralisation, whereas this protective effect was abolished by pre-treatment with GW4869 (Fig. 2K and L). These results suggest that A-EC/sEVs inhibited the osteogenic differentiation of HA-VSMCs induced by β -GP.

The miR-126-5p is highly enriched in the A-EC/sEVs

MicroRNAs (miRs), the crucial cargo of sEVs, play critical roles in regulating the function of target cells by directing the posttranscriptional repression of mRNA targets [32, 33]. Previous studies have reported a large number of endothelial-associated miRNAs, which are closely related to vascular diseases [34–39]. Therefore, we detected the expression profiles of these miRNAs by qPCR in HUVEC-derived sEVs with or without AGEs treatment. The results revealed that the levels of miR-126 were significantly up-regulated, especially the miR-126-5p level in A-EC/sEVs compared to EC/sEVs (Fig. 3A, B), but there were no significant changes in other candidate miRNAs. To confirm that the miR-126 was confined inside sEVs, the samples were treated with RNase and PK. In contrast to the control group, the level of the miRNA-126 was not impacted by the RNase and PK treatment and was degraded only when the sEVs membrane integrity was damaged with the detergent Triton X-100 (Fig. 3C). Overall, these results indicate that miR-126-5p is highly enriched in sEVs derived from AGEs induced HUVECs and may be the main effector molecule that alleviates calcification.

To evaluate whether the mature miR-126-5p in VSMCs is of HUVECs origin, both primary and mature miR-126-5p were detected simultaneously in HUVECs and HA-VSMCs by qRT-PCR. Both primary and

(See figure on next page.)

Fig. 3 A-EC/sEVs disrupted the smad1/5/9 signalling pathway by delivering miR-126-5p. **A** Heatmap showing expression profiles of candidate miRNAs. **B** Analysis by PCR showing normalized levels of candidate miRNAs. **C** The sEVs were treated or not (Con) with Triton X-100 (T) and incubated with or without RNases and PK (PK/R). miR-126 levels were measured by qPCR. **D** Venn diagram showing bioinformatics analysis of miR-126-5p target genes. **E** Luciferase reporter assays were conducted using luciferase constructs carrying a WT or mutant BMPR1B 3'-UTR co-transfected into HA-VSMCs with miR-126-5p mimics. Firefly luciferase activity was normalised to Renilla luciferase activity. Data were presented as mean \pm SD of three replicates. $^{**}P < 0.01$. **F** Expression of BMPR1B, Runx2, BMP2, t-p-smad1/5/9 and p-smad1/5/9 after transfection with miR-126-5p in calcified HA-VSMCs. **G, H** The representative image of ALP staining and ALP activity. **G, I** The representative image of ARS staining and calcium deposition. **J–K** Silencing efficiency of small interfering RNA on BMPR1B analyzed by qPCR and western blotting. **L** The protein level of t-p-smad1/5/9, intranuclear p-smad1/5/9, Runx2 and BMP2 was detected by western blotting after miR-126-5p transfection in a BMPR1B-silenced VSMC calcification model. **M** The representative image of ALP staining and ARS staining after miR-126-5p transfection in a BMPR1B-silenced VSMC calcification model. **N** ALP activity and **O** calcium deposition after miR-126-5p transfection in a BMPR1B-silenced VSMC calcification model. Data were presented as mean \pm SD of three replicates. NS, not significant

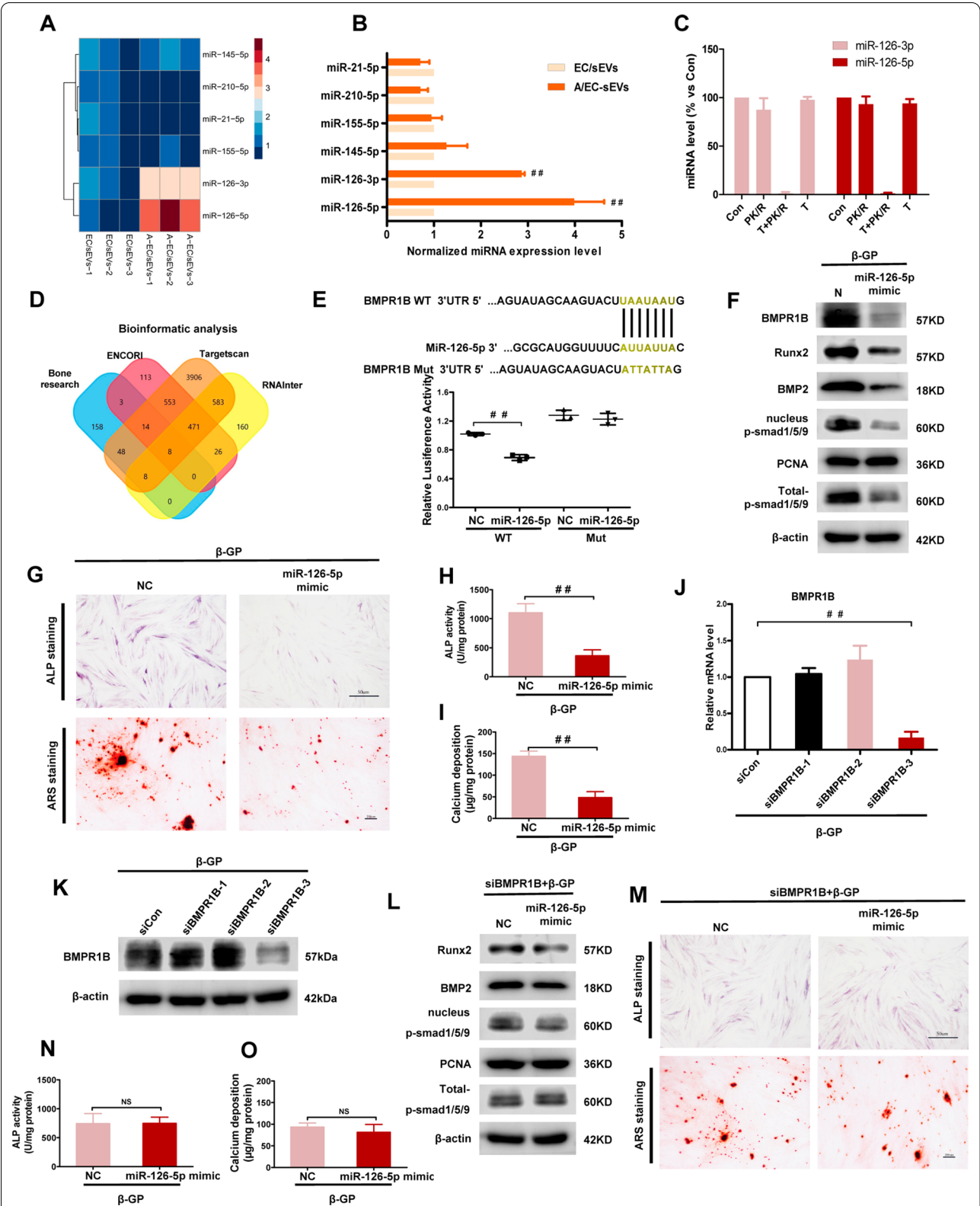


Fig. 3 (See legend on previous page.)

mature miR-126-5p were up-regulated in HUVECs treated with AGEs (Additional file 1: Fig. S4A, B). Additionally, A-EC/sEVs treatment significantly increased the level of mature miR-126-5p, but not primary miR-126-5p, in HA-VSMCs compared to the control (Additional file 1: Fig. S4C, D), suggesting that increased miR-126-5p level in VSMCs is due to the delivery of sEVs rather than endogenous production.

A-EC/sEVs-mediated anti-calcification requires miR-126-5p-BMPR1B-smad1/5/9 axis

To exploit the underlying mechanisms of the A-EC/sEVs encapsulation of miR-126-5p, we predicted the target gene of miR-126-5p using four databases (Fig. 3D). Interestingly, the bioinformatic score system revealed that bone morphogenetic protein receptor type 1B (BMPR1B) has binding sites for miR-126-5p (Fig. 3E). With respect to calcification, BMPR1B is an intriguing miRNA target, as its downstream region involves the BMP-smad signalling pathway which has been reported to play an essential role in vascular calcification [31, 40, 41]. To confirm that miR-126-5p specifically targets *BMPR1B*, we produced a luciferase reporter with a mutant *BMPR1B* 3'UTR containing the miR-126-binding site at the seed sequence (Fig. 3E). Luciferase reporter assays confirmed that miR-126 effectively targets the wild-type *BMPR1B* 3'UTR rather than the mutant *BMPR1B* 3'UTR (Fig. 3E). Consistent with the bioinformatic analysis, BMPR1B transcript and protein levels were strongly down-regulated by miR-126-5p overexpression (Fig. 3F, Additional file 1: Fig. S5). Accordingly, miR-126-5p overexpression was sufficient to decrease the protein level of Runx2, BMP2 (Fig. 3F) and ALP, as well as calcium deposition (Fig. 3G–I). Interestingly, miR-126-5p overexpression reduced the level of total phosphorylated smad1/5/9 (total-p-smad1/5/9) and nucleus p-smad1/5/9 (Fig. 3F). In line with this, A-EC/sEVs also significantly down-regulated levels of BMPR1B, total-p-smad1/5/9 and intranuclear p-smad1/5/9 (Additional file 1: Fig. S6A, B).

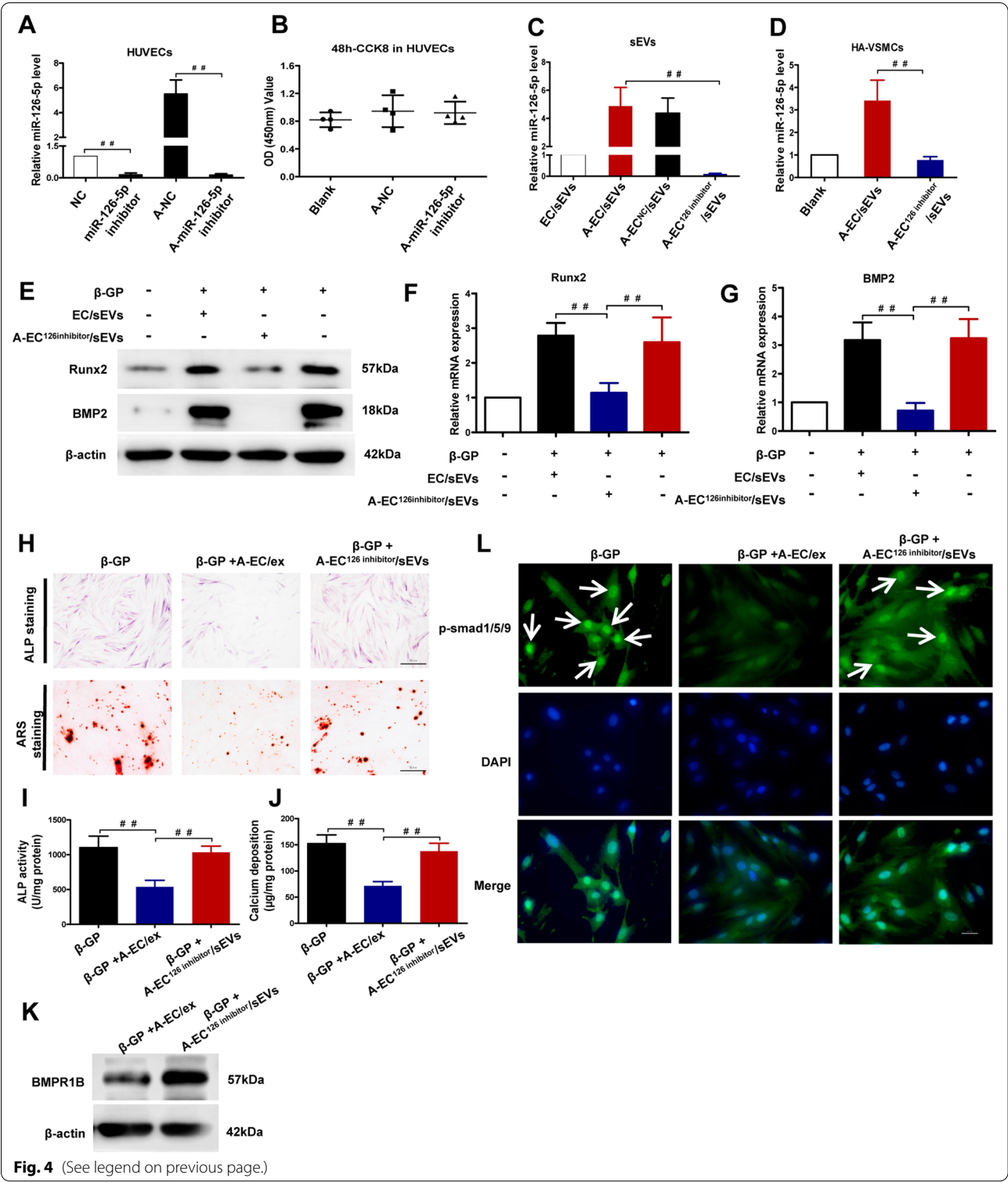
To test the role of BMPR1B-mediated effects on miR-126-5p, we knocked-down BMPR1B expression using RNA interference (RNAi). The small interference RNA of BMPR1B (siBMPR1B) with the best silencing efficiency was selected for the next experiment. siBMPR1B-3 markedly down-regulated BMPR1B transcript and protein levels (Fig. 3H–J). As expected, we found that miR-126-5p overexpression no longer has the effect of anti-calcification after the silencing of BMPR1B in VSMCs (Fig. 3L–O). In line with this, A-EC/sEVs lost their anti-calcification effects in the BMPR1B-silenced VSMCs model (Additional file 1: Fig. S7A–D). Together, these results indicate that the miR-126-5p-BMPR1B-smad1/5/9 axis is necessary for A-EC/sEVs-mediated anti-calcification.

MiR-126-5p silencing blunts A-EC/sEVs-mediated anti-calcification in vitro by restoring the activation of the BMP/smud1/5/9 signalling pathway

To verify the predominant role of miR-126-5p in A-EC/sEV-mediated anti-calcification in vitro, we prevented miR-126-5p from being enriched in vesicles. As shown in Fig. 4A, the transfection of the miRNA-126-5p inhibitor dramatically reduced the level of miR-126-5p in HUVECs compared to the control group. Then, we used AGEs to stimulate HUVECs transfected with the negative control (NC) or the miR-126-5p inhibitor. The results showed that AGEs treatment significantly enhanced the level of miR-126-5p in the NC group but not in the miR-126-5p inhibitor group (Fig. 4A). Moreover, treatment with AGEs and the miR-126-5p inhibitor did not affect the viability of HUVECs (Fig. 4B). sEVs were isolated from the NC or miR-126-5p inhibitor group treated with AGEs, termed A-EC^{NC}/sEVs and A-EC^{126inhibitor}/sEVs, respectively. The level of miR-126-5p in A-EC^{126inhibitor}/sEVs was significantly lower than that in A-EC/sEVs (Fig. 4C), suggesting that miR-126-5p silencing means that AGEs stimulated HUVEC-derived sEVs no longer carry abundant miR-126-5p. Consistently, A-EC^{126inhibitor}/sEVs treatment did

(See figure on next page.)

Fig. 4 miR-126-5p silencing reversed A-EC/sEVs-mediated anti-calcification effects on VSMCs by restoring the activation of smad1/5/9 signalling. We transfected miR-126-5p inhibitor to silence miR-126-5p expression in HUVEC with or without AGEs treatment, including 4 groups: negative control (NC), miR-126-5p inhibitor, A-NC, A-miR-126-5p inhibitor. **A** The transfection efficiency examined by qPCR in HUVECs. **B** CCK-8 assay showing the viability of HUVECs after 48 h co-incubation. ^{##}P < 0.01. Data were presented as mean ± SD of 3 replicates. We isolated sEVs from the A-NC or A-miR-126-5p inhibitor group, termed A-EC^{NC}/sEVs or A-EC^{126inhibitor}/sEVs, respectively. **C** Analysis by qPCR showing the level of miR-126-5p in four sEVs (EC/sEVs, A-EC/sEVs, A-EC^{NC}/sEVs or A-EC^{126inhibitor}/sEVs). ^{##}P < 0.01; data were presented as the mean ± SD of three replicates. **D** Analysis by qPCR showing the level of miR-126-5p in HA-VSMCs treated with A-EC/sEVs or A-EC^{126inhibitor}/sEVs. **E–G** The mRNA and protein level of Runx2 and BMP2 in calcified HA-VSMCs treated with A-EC/sEVs or A-EC^{126inhibitor}/sEVs. **H** ALP staining and ARS staining of calcified HA-VSMCs treated with A-EC/sEVs or A-EC^{126inhibitor}/sEVs. Representative micrographs are shown, scale bar represents 50 µm. **I, J** ALP activity and calcium content of calcified HA-VSMCs treated with A-EC/sEVs or A-EC^{126inhibitor}/sEVs. ^{##}P < 0.01. **K** The protein level of BMPR1B in calcified HA-VSMCs treated with A-EC/sEVs or A-EC^{126inhibitor}/sEVs. **L** Representative fluorescence micrographs showing the nuclear translocation of p-smad1/5/9 (green) in calcified HA-VSMCs treated with A-EC/sEVs or A-EC^{126inhibitor}/sEVs. Nuclei were counterstained with DAPI (blue). Scale bar represents 50 µm



not affect the level of miR-126-5p in HA-VSMCs compared to A-EC/sEVs (Fig. 4D). Next, we sought to evaluate whether A-EC^{126inhibitor}/sEVs abolished the anti-calcification effect. Compared to the A-EC/sEVs group, A-EC^{126inhibitor}/sEVs no longer down-regulated the Runx2 and BMP2 expression (Fig. 4E–G), ALP activity and mineralisation (Fig. 4H–J). Subsequently, we investigated whether miR-126-5p

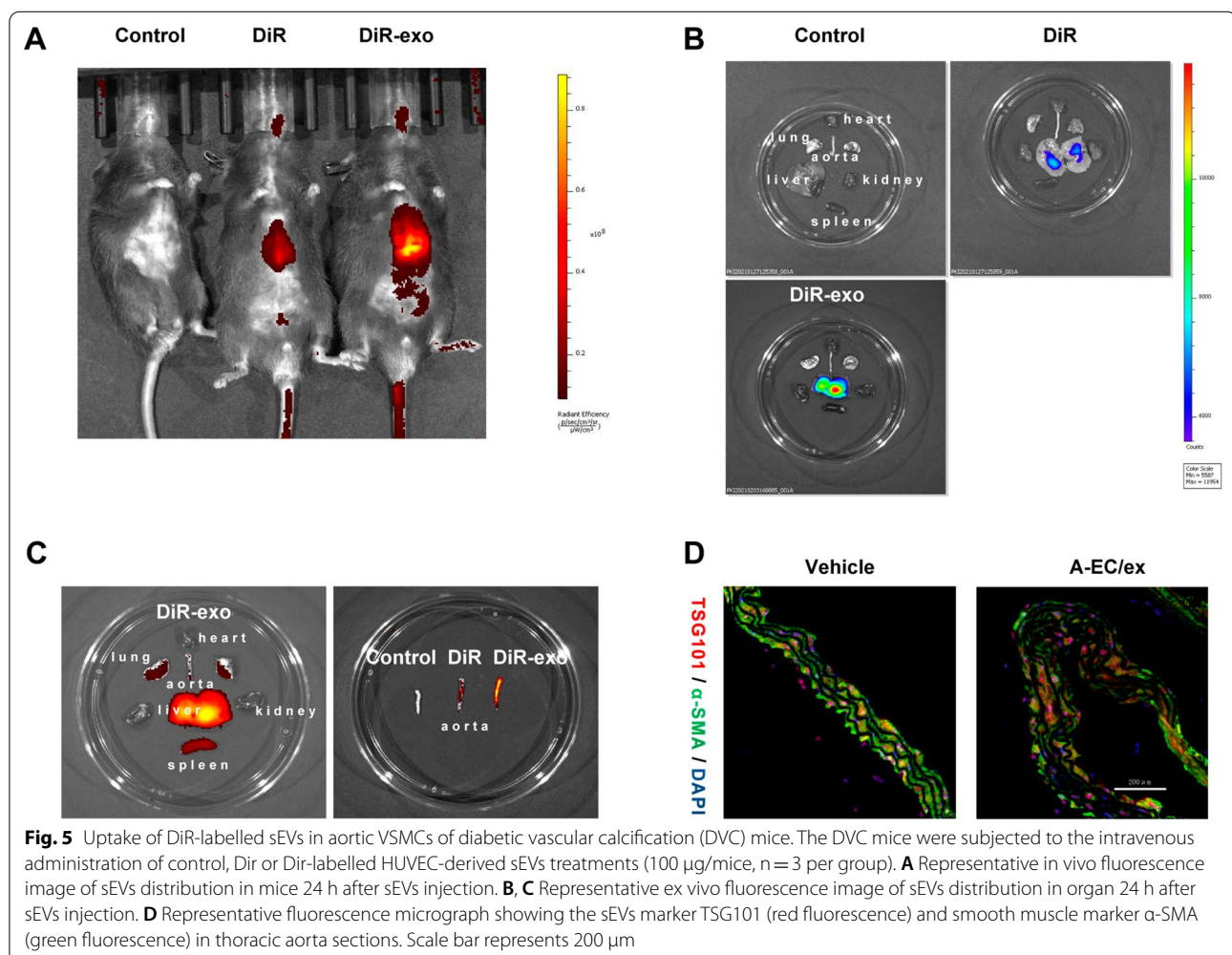
silencing influenced the downstream BMP/smad1/5/9 signalling pathway. Compared to the A-EC/sEVs group, A-EC^{126inhibitor}/sEVs no longer reduced BMPR1B expression, p-smad1/5/9 or its nuclear translocation (Fig. 4K, L). Together, the data indicated that miR-126-5p silencing partially reversed A-EC/sEVs-mediated anti-calcification in vitro by restoring activation of the BMP/smad1/5/9 signalling pathway.

A-EC/sEVs prevent vascular calcification in vivo involving miR-126-5p-BMPR1B-smad1/5/9

To determine whether A-EC/sEVs could be incorporated by aortic VSMCs in vivo, DiR-labelled sEVs were injected into mice through the tail vein to track their distribution. Using the control mice as a reference, the fluorescence intensity was adjusted to exclude the interference of autofluorescence. The results showed that we successfully injected the DiR-labeled sEVs into the mice through the tail vein (Fig. 5A, B). The fluorescence was mainly distributed in the liver, lung, aorta and spleen tissues (Fig. 5C).

Moreover, injection of sEVs significantly increased the expression of the exosomal marker TSG101 in VSMCs of the aorta (Fig. 5D). These results indicate that the exogenous HUVEC-derived sEVs were successfully injected into mice and then they were taken up by VSMCs in the aorta.

To demonstrate whether A-EC/sEVs antagonise vascular calcification in vivo, a diabetic mouse model was established by feeding with a high-fat diet combined with the intraperitoneal injection of STZ [42]. Then, type 2 diabetic mice (T2D) were injected intraperitoneally with vitamin D2 to establish a diabetic vascular calcification (DVC) model [43]. DVC mice presented random blood glucose levels higher than 16.7 mmol/L, while levels in the normal group were lower than 9 mmol/L (Additional file 1: Fig. S8). Three kinds of extracellular vesicles (EC/sEVs, A-EC/sEVs and A-EC^{126inhibitor}/sEVs) and vehicle were injected into DVC mice through tail vein (Fig. 6A). Consistently, A-EC/sEVs treatment dramatically up-regulated miR-126-5p expression in the aorta



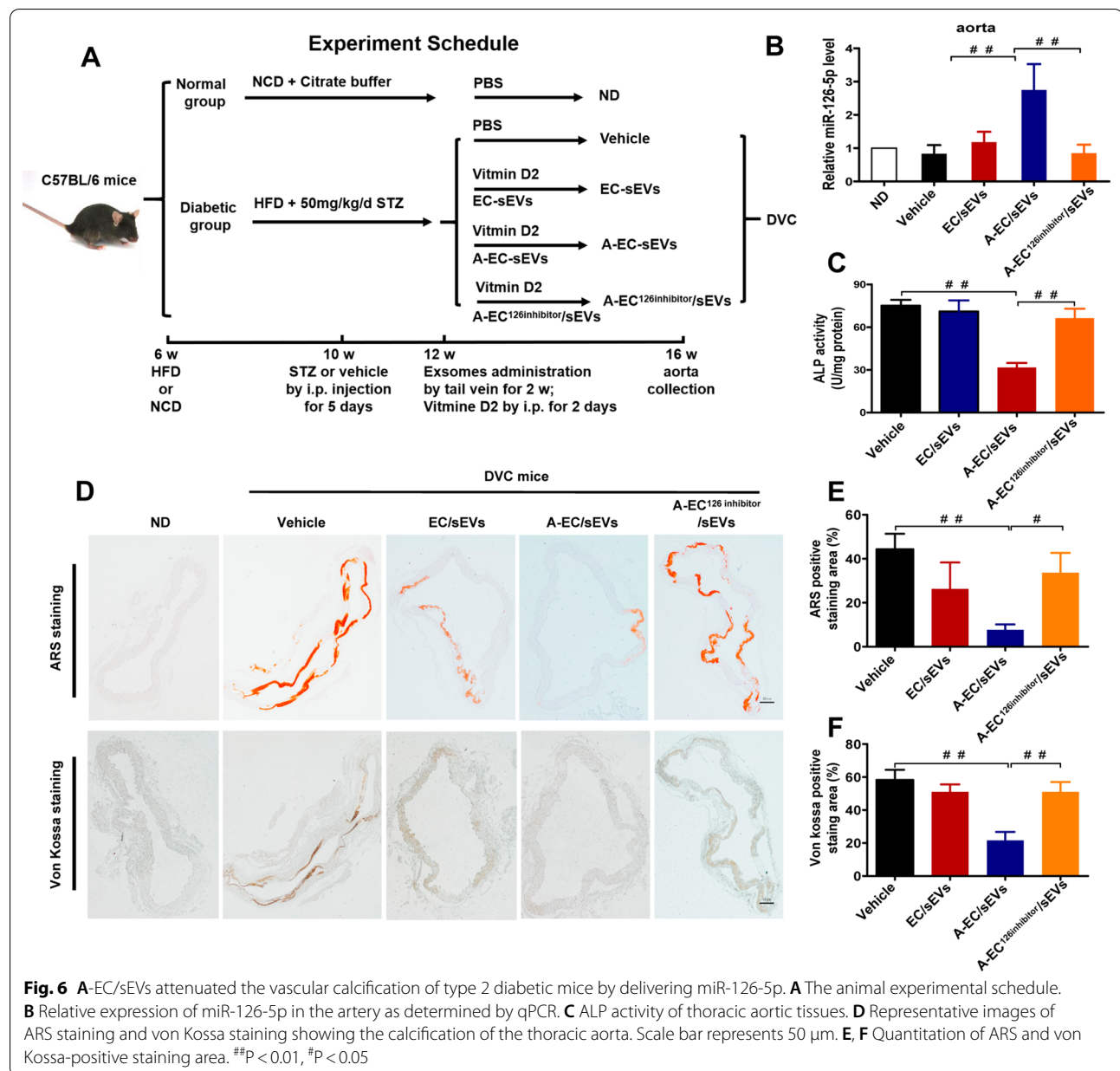
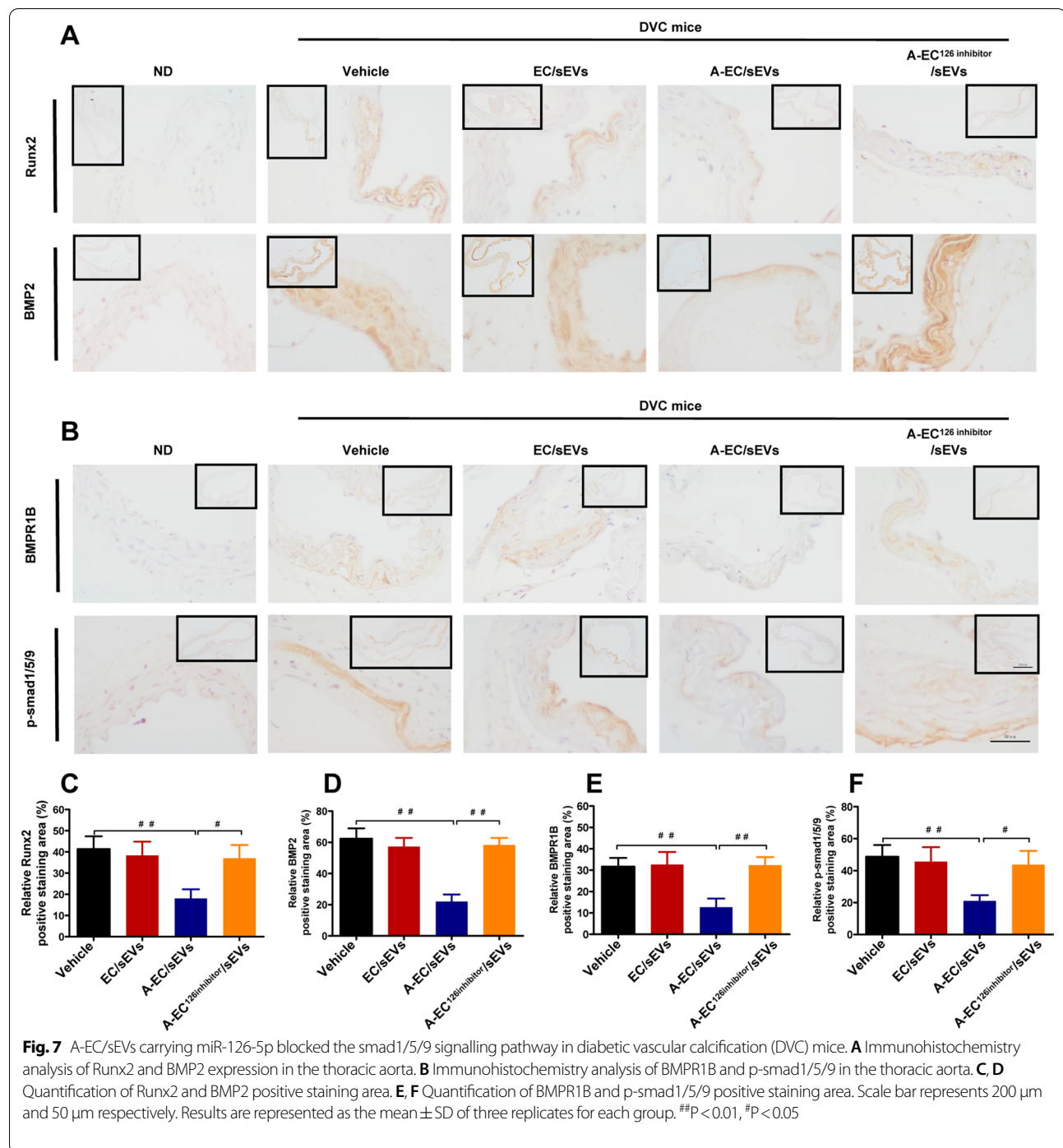


Fig. 6 A-EC/sEVs attenuated the vascular calcification of type 2 diabetic mice by delivering miR-126-5p. **A** The animal experimental schedule. **B** Relative expression of miR-126-5p in the artery as determined by qPCR. **C** ALP activity of thoracic aortic tissues. **D** Representative images of ARS staining and von Kossa staining showing the calcification of the thoracic aorta. Scale bar represents 50 μ m. **E, F** Quantitation of ARS and von Kossa-positive staining area. $^{##}P < 0.01$, $^{*}P < 0.05$

after the administration of exogenous sEVs compared to EC/sEVs and A-EC^{126inhibitor}/sEVs treatment partially abolished this effect (Fig. 6B). As expected, the thoracic aorta of DVC mice had significantly higher ALP activity (Fig. 6C), calcification (Fig. 6D–F) and levels of RUNX2 and BMP2 (Fig. 7A, C and D) compared to animals in the ND group, suggesting the successful establishment of a diabetic vascular calcification model. A-EC/sEVs treatment significantly reduced ALP activity (Fig. 6C), calcification (Fig. 6D–F) and RUNX2 and BMP2 expression (Fig. 7A, C and D) in the thoracic aorta of DVC mice

when compared to the EC/sEVs group and treatment with A-EC^{126inhibitor}/sEVs reversed these effects. The results strongly support that fact that A-EC/sEVs encapsulating miR-126-5p could be internalised into mouse VSMCs, thus preventing vascular calcification in DVC mice. Immunohistochemical staining was performed to evaluate the expression of BMPR1B and p-smad1/5/9 in the thoracic aorta. The micrograph showed that A-EC/sEVs treatment reduced the expression of BMPR1B and p-smad1/5/9 in DVC mice when compared to the EC/sEVs group, but treatment with A-EC^{126inhibitor}/sEVs



reversed this effect (Fig. 7B, E and F). Collectively, these data demonstrate that protective effect of A-EC/sEVs on the vascular calcification in vivo involving miR-126-5p-BMPR1B-smad1/5/9.

Discussion

Herein, we provide evidence for a novel communication mechanism between ECs and VSMCs under the stimulus of AGEs. Specifically, sEVs isolated from AGEs

stimulated HUVECs could attenuate vascular calcification associated with diabetes. We found that this mechanism was partially mediated by exosomal miR-126-5p, which was secreted by AGEs stimulated HUVECs and delivered into VSMCs, particularly targeting the 3'UTR of *BMPR1B*, thereby disrupting the smad1/5/9 signalling pathway and regulating the expression of the osteogenic gene. Thus, these findings support a potential role of miR-126-5p in treating media calcification in diabetic patients.

Aortic calcification is a common vascular complication in patients with diabetes, mainly involving the middle layer of the aorta [3]. However, no effective strategies have been proposed to inhibit vascular media calcification in diabetic patients at present. EVs are an important nanomedicine with many potential applications due to their high stability, accessibility and rich sources compared to traditional medicine for a variety of different diseases [44–50]. Recently, several studies have reported that HUVEC-derived EVs attenuate apoptosis in neurons suffering from oxygen–glucose deprivation [20] and promote an antitumour response in malignant mesothelioma by transferring miR-126 [51]. Intriguingly, sEVs from HUVECs under hypoxia/reoxygenation (H/R) conditions were found to display the same protective effects on neurons under H/R stimulation as HUVEC-derived EVs [52, 53]. These results demonstrated the beneficial effects of the therapeutic potential of HUVEC-derived EVs on some disease status. It is reported that HUVEC-derived sEVs decreased the expression of contractile phenotype marker genes such as α -SMA, smoothelin and calponin in SMCs [54]. However, the role of HUVEC-derived sEVs in the transdifferentiation of VSMCs from a contractile to osteogenic phenotype, which is a major pathogenetic mechanism of aortic calcification, remains unknown. Unexpectedly, our in vivo and in vitro experiments showed that HUVEC-derived EVs did not affect vascular calcification. Therefore, we preliminarily excluded the therapeutic potential of HUVEC-derived sEVs itself.

Advanced glycation end-products are produced by the non-enzymatic reaction of reducing sugars with the amino groups of proteins, lipids and nucleic acids through a series of reactions known as the Maillard reaction [54]. Normally, AGEs slowly increase in non-diabetic subjects, as they can be ingested exogenously through tobacco and certain foods, especially heated foods [55]. However, in diabetic patients, AGEs are produced and accumulate rapidly due to high blood glucose levels in the circulation [56]. The excess accumulation of AGEs in a variety of tissues accelerate the progression of the disease [57, 58]. Interestingly, AGEs activated ECs, resulting in EC dysfunction [25], but the activated or apoptotic

ECs-secreted EVs carrying protective molecules to protect them against apoptosis and promote EC repair [25]. Consistent with this, the data in the present study demonstrated that sEVs from AGEs stimulated HUVECs were able to inhibit the osteogenic differentiation of VSMCs, as evidenced by the reductions in ALP activity, BMP2 and Runx2 expression and calcium deposition. Similarly, another researcher reported that sEVs from AGEs stimulated MSCs inhibited the osteogenic differentiation of VSMCs [41]. These results seem to suggest that AGEs may have a beneficial effect on vascular calcification by stimulating the secretion of sEVs by endothelial cells, probably as each coin has two sides. Nevertheless, the detrimental effects of AGEs cannot be ignored in patients with diabetes.

MicroRNAs transferred by sEVs from derived cells to recipient cells bind to the 3'UTR of target mRNA, leading to their degradation or the repression of translation, thereby regulating the function of target cells [33]. In this study, we found that the anti-calcification effect of sEVs from AGEs stimulated HUVECs may be attributed to its encapsulated main cargo, miR-126-5p. The level of miR-126-3p in sEVs also increased slightly, but the degree of increase was significantly lower than that of miR-126-5p. miR-126-3p has been reported to mediate the anti-calcification effect of ERK1/2 inhibitors [59], but the role of miR-126-5p has never been investigated. Mature miR-126-5p and miR-126-3p represent miRNAs processed from the 5' and 3' ends of pri-mir-126, respectively [60–62]. We ruled out the possibility that the target cells themselves produce mature miR-126 and proved that the anti-calcification effect of EVs is through the transfer of miR-126 mature to the target cells. In order to eliminate the effect of miR-126-3p elevation in sEVs, we directly overexpressed miR-126-5p in target cells and proved the anti-calcification effect of miR-126-5p. Consistent with our results, a new study reported that ECs-specific microRNA-126 knockout mice exhibited excessive accumulation of calcium [63]. These evidences suggest that the pivotal role of miR-126 in vascular calcification cannot be ignored.

We further identified *BMPR1B* as the important target gene of miR-126-5p by luciferase reporter assays. Consistently, the overexpression of miR-126-5p in target cells down regulated the transcription and translation levels of *BMPR1B*. *BMPR1B* is an essential receptor of the BMP/smad1/5/9 signalling pathway [64], which has been reported to promote osteogenic differentiation by regulating the expression of osteogenic genes [40, 65, 66]. Accordingly, the down-regulation of *BMPR1B1b* by RNAi technology inhibited the phosphorylation and nuclear translocation of its

downstream p-smad1/5/9 and reduced the expression of osteogenic genes, thus decreasing vascular calcification in T2D mice. In contrast, miR-126-5p silencing in A-EC/sEVs almost reversed these effects. Furthermore, we confirmed that both miR-126-5p overexpression and A-EC/sEVs treatment lost their anti-calcification effects in the BMPR1B-silenced cell model. Taken together, miR-126-5p-enriched A-EC/sEVs inhibited the calcification of VSMCs by down-regulating the expression of *BMPR1B*, thereby blocking the smad1/5/9 signalling pathway. This contributes to our understanding of the pathogenic mechanism of media calcification in diabetic patients and provides directions for the identification of new therapeutic targets.

Conclusion

In vitro and in vivo results indicate that sEVs secreted by AGEs stimulated HUVECs are rich in miR-126-5p, which inhibits diabetic media calcification by blocking the smad1/5/9 signalling pathway. Our findings suggest that the use of nanomedicine combined with miR-126-5p may be a promising therapeutic approach to prevent vascular calcification in diabetic patients.

Abbreviations

AGEs: Advanced glycation end products; ALP: Alkaline Phosphatase; ARS: Alizarin Red staining; BMP2: BMP2 bone morphogenetic protein 2; BMPR1B: Bone morphogenetic protein receptor type 1B; DM: Diabetes mellitus; ECs: Endothelial cells; sEVs: Small extracellular vesicles; HUVECs: Human umbilical vein endothelial cells; H/R Hypoxia/reoxygenation; miRNAs: MicroRNAs; MSCs: Mesenchymal stromal cells; PK: Proteinase K; RUNX2: RUNX family transcription factor 2; SMAD1/5/9: Family member 1, 5, and 9 STZ Streptozotocin T2D Type 2 diabetic; VC: Vascular calcification; VSMCs: Vascular smooth muscle cells; β -GP: β -Glycerophosphate.

Supplementary Information

The online version contains supplementary material available at <https://doi.org/10.1186/s12951-022-01529-z>.

Additional file 1: Fig. S1. AGEs Reduce the Viability of HUVEC in a Dose/Time-Dependent Manner. **Fig. S2** Identification of HA-VSMCs. **Fig. S3.** AGEs-stimulated HUVECs reduce the protein level of Runx2 and BMP2 in VSMCs by secreting sEVs rather than other soluble mediators. **Fig. S4.** miR-126-5p was delivered into VSMCs by sEVs. **Fig. S5.** miR-126-5p overexpression significantly reduced the transcript level of BMPR1B. **Fig. S6.** A-EC/sEVs decreased BMPR1B expression and phosphorylation and nuclear translocation of smad1/5/9 in calcified HA-VSMCs. **Fig. S7.** A-EC/sEVs did not affect levels of Runx2, BMP2, total-p-smad1/5/9 and intranuclear p-smad1/5/9 in BMPR1B-silenced HA-VSMCs. **Fig. S8.** Random blood glucose levels of ND and DVC mice.

Acknowledgements

We are very grateful to Tongtian Zhuang for his help.

Author contributions

L-QY and BG conceived and designed the experiments. BG performed the experiments and prepared the figures. YW, Q-SX, M-HZ, L-ML analysed the data. X-BL, FX, XL, and F-X-L, FW, S-KS provided technical support. L-QY and BG wrote the manuscript. C-CL, Z-AZ, MHEU revised the manuscript. All authors read and approved the final manuscript.

Funding

This work was supported by the National Natural Science Foundation of China (Grant Numbers 81770881, 81870623, 82070910), the Fundamental Research Funds for Central Universities of Central South University (2021zzts0387), Key R&D Plan of Hunan Province (2020SK2078) and the Natural Science Foundation of Hunan Province (2021JJ30036).

Availability of data and materials

The data supporting the conclusions of this article are included within the article and its supplementary information.

Declarations

Ethics approval and consent to participate

All experiments were reviewed and approved by the Ethics Committee of the Second Xiang-Ya Hospital, Central South University (2020338).

Consent for publication

Not applicable.

Competing interests

The authors declare that they have no competing interests.

Author details

¹National Clinical Research Center for Metabolic Diseases, Department of Metabolism and Endocrinology, The Second Xiangya Hospital, Central South University, Changsha 410000, China. ²Department of Radiology, The Second Xiangya Hospital, Central South University, Changsha, Hunan, People's Republic of China. ³Department of Pathology, The Second Xiangya Hospital, Central South University, Changsha, Hunan, People's Republic of China.

⁴Department of Cardiovascular Surgery, The Second Xiangya Hospital, Central South University, Changsha, Hunan, People's Republic of China.

Received: 15 December 2021 Accepted: 28 June 2022

Published online: 16 July 2022

References

- Sun H, Saeedi P, Karuranga S, Pinkepank M, Ogurtsova K, Duncan BB, Stein C, Basit A, Chan J, Mbanya JC, Pavkov ME, Ramachandran A, Wild SH, James S, Herman WH, Zhang P, Bommer C, Kuo S, Boyko EJ, Magliano DJ. IDF Diabetes Atlas: Global, regional and country-level diabetes prevalence estimates for 2021 and projections for 2045. *Diabetes Res Clin Pract.* 2022;183: 109119. <https://doi.org/10.1016/j.diabres.2021.109119>.
- Williams R, Karuranga S, Malanda B, Saeedi P, Basit A, Besancon S, Bommer C, Esteghamati A, Ogurtsova K, Zhang P, Colagiuri S. Global and regional estimates and projections of diabetes-related health expenditure: results from the International Diabetes Federation Diabetes Atlas, 9th edition. *Diabetes Res Clin Pract.* 2020;162: 108072. <https://doi.org/10.1016/j.diabres.2020.108072>.
- Lanzer P, Hannan FM, Lanzer JD, Janzen J, Raggi P, Furniss D, Schuchardt M, Thakker R, Fok PW, Saez-Rodriguez J, Millan A, Sato Y, Ferraresi R, Virmani R, St HC. Medial arterial calcification: JACC state-of-the-art review. *J Am Coll Cardiol.* 2021;78(11):1145–65. <https://doi.org/10.1016/j.jacc.2021.06.049>.
- Williams MC, Abbas A, Tirr E, Alam S, Nicol E, Shambrook J, Schmitt M, Hughes GM, Stirrup J, Holloway B, Gopalan D, Deshpande A, Weir-McCall J, Agrawal B, Rodrigues J, Brady A, Roditi G, Robinson G, Bull R. Reporting incidental coronary, aortic valve and cardiac calcification on non-gated thoracic computed tomography, a consensus statement from the BSCI/ BSCCT and BSTI. *Br J Radiol.* 2021;94(1117):20200894. <https://doi.org/10.1259/bjr.20200894>.
- Thery C, Witwer KW, Aikawa E, Alcaraz MJ, Anderson JD, Andriantsitohaina R, Antoniou A, Arab T, Archer F, Atkin-Smith GK, Ayre DC, Bach JM, Bachurski D, Baharvand H, Balaj L, Baldacchino S, Bauer NN, Baxter AA, Bebawy M, Beckham C, Bedina ZA, Benmoussa A, Berardi AC, Bergese P, Bielska E, Blenkiron C, Bobis-Wozowicz S, Boilard E, Boireau W, Bongiovanni A, Borrás FE, Bosch S, Boulanger CM, Breakefield X, Breglio AM, Brennan MA, Brigstock DR, Brisson A, Broekman ML, Bromberg JF, Bryl-Gorecka P, Buch

- S, Buck AH, Burger D, Busatto S, Buschmann D, Bussolati B, Buzas EI, Byrd JB, Camussi G, Carter DR, Caruso S, Chamley LW, Chang YT, Chen C, Chen S, Cheng L, Chin AR, Clayton A, Clerici SP, Cocks A, Cocucci E, Coffey RJ, Cordeiro-da-Silva A, Couch Y, Coumans FA, Coyle B, Crescitelli R, Criado MF, D'Souza-Schorey C, Das S, Datta CA, de Candia P, De Santana EF, De Wever O, Del PH, Demaret T, Deville S, Devitt A, Dhondt B, Di Vizio D, Dieterich LC, Dolo V, Dominguez RA, Dominici M, Dourado MR, Driedonks TA, Duarte FV, Duncan HM, Eichenberger RM, Ekstrom K, El AS, Elie-Caille C, Erdbrugger U, Falcon-Perez JM, Fatima F, Fish JE, Flores-Bellver M, Forsonits A, Frelet-Barrand A, Fricke F, Fuhrmann G, Gabrielson S, Gamez-Valero A, Gardiner C, Gartner K, Gaudin R, Gho YS, Giebel B, Gilbert C, Gimona M, Giusti I, Goberdhan DC, Gorgens A, Gorski SM, Greening DW, Gross JC, Gualerzi A, Gupta GN, Gustafson D, Handberg A, Haraszi RA, Harrison P, Hegyesi H, Hendrix A, Hill AF, Hochberg FH, Hoffmann KF, Holder B, Holthofer H, Hosseinkhani B, Hu G, Huang Y, Huber V, Hunt S, Ibrahim AG, Ikezu T, Inal JM, Isin M, Ivanova A, Jackson HK, Jacobsen S, Jay SM, Jayachandran M, Jenster G, Jiang L, Johnson SM, Jones JC, Jong A, Jovanovic-Talisman T, Jung S, Kalluri R, Kano SI, Kaur S, Kawamura Y, Keller ET, Khamari D, Khomyakova E, Khvorova A, Kierulff P, Kim KP, Kislinger T, Klingeborn M, Klinken DN, Kornek M, Kosanovic MM, Kovacs AJ, Kramer-Albers EM, Krasemann S, Krause M, Kurochkin IV, Kusuma GD, Kuypers S, Laitinen S, Langevin SM, Languino LR, Lannigan J, Lasser C, Laurent LC, Lavieu G, Lazaro-Ibanez E, Le Lay S, Lee MS, Lee Y, Lemos DS, Lenassi M, Leszczynska A, Li IT, Liao K, Libregts SF, Ligeti E, Lim R, Lim SK, Line A, Linnemannstons K, Llorente A, Lombard CA, Lorenowicz MJ, Lorincz AM, Lotvall J, Lovett J, Lowry MC, Loyer X, Lu Q, Lukomska B, Lunavat TR, Maas SL, Malhi H, Marcilla A, Mariani J, Mariscal J, Martens-Uzunova ES, Martin-Jaulier L, Martinez MC, Martins VR, Mathieu N, Mathivanan S, Maugeri M, McGinnis LK, McVey MJ, Meckes DJ, Meehan KL, Mertens I, Minciacci VR, Moller A, Moller JM, Morales-Kastresana A, Morhayim J, Mullier F, Muraca M, Musante L, Mussack V, Muth DC, Myburgh KH, Najrana T, Nawaz M, Nazarenko I, Nejsum P, Neri C, Neri T, Nieuwland R, Nimrichter L, Nolan JP, Nolte-T HE, Noren HN, O'Driscoll L, O'Grady T, O'Loughlin A, Ochiya T, Olivier M, Ortiz A, Ortiz LA, Osteoetxea X, Ostergaard O, Ostrowski M, Park J, Pegtel DM, Peinado H, Perut P, Pfaffl MW, Phinney DG, Pieters BC, Pink RC, Pisetsky DS, Pogge VSE, Polakovicova I, Poon IK, Powell BH, Prada I, Pulliam L, Quesenberry P, Radeghieri A, Raffai RL, Raimondo S, Rak J, Ramirez MI, Raposo G, Rayyan MS, Regev-Rudski N, Ricklefs FL, Robbins PD, Roberts DD, Rodrigues SC, Rohde E, Rome S, Rouschop KM, Ruggeri A, Russell AE, Saa P, Sahoo S, Salas-Huenuleo E, Sanchez C, Saugstad JA, Saul MJ, Schiffelers RM, Schneider R, Schoyen TH, Scott A, Shahaj E, Sharma S, Shatnyeva O, Shekari F, Shelke GV, Shetty AK, Shiba K, Siljander PR, Silva AM, Skowronek A, Snyder ON, Soares RP, Sodar BW, Soekmadji C, Stollito J, Stahl PD, Stoorvogel W, Stott SL, Strasser EF, Swift S, Tahara H, Tewari M, Timms K, Tiwari S, Tixeira R, Tkach M, Toh WS, Tomasini R, Torrecillas AC, Tosar JP, Toxavidis V, Urbanelli L, Vader P, van Balkom BW, van der Grein SG, Van Deun J, van Herwijnen MJ, Van Keuren-Jensen K, van Niel G, van Royen ME, van Wijnen AJ, Vasconcelos MH, Vechetti JJ, Veit TD, Vella LJ, Velot E, Verweij FJ, Vestad B, Vinas JL, Visnovitz T, Vukman KV, Wahlgren J, Watson DC, Wauben MH, Weaver A, Webber JP, Weber V, Wehman AM, Weiss DJ, Welsh JA, Wendt S, Wheelock AM, Wiener Z, Witte L, Wolfram J, Xagorari A, Xander P, Xu J, Yan X, Yanez-Mo M, Yin H, Yuana Y, Zappulli V, Zarubova J, Zekas V, Zhang JY, Zhao Z, Zheng L, Zheutlin AR, Zickler AM, Zimmermann P, Zivkovic AM, Zocco D, Zuba-Surma EK. Minimal information for studies of extracellular vesicles 2018 (MISEV2018): a position statement of the International Society for Extracellular Vesicles and update of the MISEV2014 guidelines. *J Extracell Vesicles*. 2018;7(1):1535750. <https://doi.org/10.1080/20013078.2018.1535750>.
6. Kalluri S, LeBleu VS, Sugimoto H, Yang S, Ruivo CF, Melo SA, Lee JJ, Kalluri R. Exosomes facilitate therapeutic targeting of oncogenic KRAS in pancreatic cancer. *Nature*. 2017;546(7659):498–503. <https://doi.org/10.1038/nature22341>.
 7. Buscail L. Pancreatic cancer: exosomes for targeting KRAS in the treatment of pancreatic cancer. *Nat Rev Gastroenterol Hepatol*. 2017;14(1):636–8. <https://doi.org/10.1038/nrgastro.2017.113>.
 8. Mathieu M, Martin-Jaulier L, Lavieu G, Thery C. Specificities of secretion and uptake of exosomes and other extracellular vesicles for cell-to-cell communication. *Nat Cell Biol*. 2019;21(1):9–17. <https://doi.org/10.1038/s41556-018-0250-9>.
 9. Wang Y, Xu F, Zhong JY, Lin X, Shan SK, Guo B, Zheng MH, Yuan LQ. Exosomes as mediators of cell-to-cell communication in thyroid disease. *Int J Endocrinol*. 2020;2020:4378345. <https://doi.org/10.1155/2020/4378345>.
 10. Isaac R, Reis F, Ying W, Olefsky JM. Exosomes as mediators of intercellular crosstalk in metabolism. *Cell Metab*. 2021;33(9):1744–62. <https://doi.org/10.1016/j.cmet.2021.08.006>.
 11. Costa VH, Gitz-Francois JJ, Schiffelers RM, Vader P. Cellular uptake of extracellular vesicles is mediated by clathrin-independent endocytosis and macropinocytosis. *J Control Release*. 2017;266:100–8. <https://doi.org/10.1016/j.jconrel.2017.09.019>.
 12. Joshi BS, de Beer MA, Giepmans B, Zuhorn IS. Endocytosis of extracellular vesicles and release of their cargo from endosomes. *ACS Nano*. 2020;14(4):4444–55. <https://doi.org/10.1021/acs.nano.9b10033>.
 13. Tkach M, Thery C. Communication by extracellular vesicles: where we are and where we need to go. *Cell*. 2016;164(6):1226–32. <https://doi.org/10.1016/j.cell.2016.01.043>.
 14. Azparren-Angulo M, Royo F, Gonzalez E, Liebana M, Brotons B, Berganza J, Goni-de-Cerio F, Manicardi N, Abad-Jorda L, Gracia-Sancho J, Falcon-Perez JM. Extracellular vesicles in hepatology: physiological role, involvement in pathogenesis, and therapeutic opportunities. *Pharmacol Ther*. 2021;218:107683. <https://doi.org/10.1016/j.pharmthera.2020.107683>.
 15. Yin Y, Chen H, Wang Y, Zhang L, Wang X. Roles of extracellular vesicles in the aging microenvironment and age-related diseases. *J Extracell Vesicles*. 2021;10(12): e12154. <https://doi.org/10.1002/jev2.12154>.
 16. Wei Y, Wu Y, Zhao R, Zhang K, Midgley AC, Kong D, Li Z, Zhao Q. MSC-derived sEVs enhance patency and inhibit calcification of synthetic vascular grafts by immunomodulation in a rat model of hyperlipidemia. *Biomaterials*. 2019;204:13–24. <https://doi.org/10.1016/j.biomaterials.2019.01.049>.
 17. Yuan K, Shamskhov EA, Orcholski ME, Nathan A, Reddy S, Honda H, Mani V, Zeng Y, Ozen MO, Wang L, Demirci U, Tian W, Nicolls MR, de Jesus PV. Loss of endothelium-derived Wnt5a is associated with reduced pericyte recruitment and small vessel loss in pulmonary arterial hypertension. *Circulation*. 2019;139(14):1710–24. <https://doi.org/10.1161/CIRCULATIONAHA.118.037642>.
 18. Yue Y, Wang C, Benedict C, Huang G, Truongcao M, Roy R, Cimini M, Garikipati V, Cheng Z, Koch WJ, Kishore R. Interleukin-10 deficiency alters endothelial progenitor cell-derived exosome reparative effect on myocardial repair via integrin-linked kinase enrichment. *Circ Res*. 2020;126(3):315–29. <https://doi.org/10.1161/CIRCRESAHA.119.315829>.
 19. Cines DB, Pollak ES, Buck CA, Loscalzo J, Zimmerman GA, McEver RP, Pober JS, Wick TM, Konkle BA, Schwartz BS, Barnathan ES, McCrae KR, Hug BA, Schmidt AM, Stern DM. Endothelial cells in physiology and in the pathophysiology of vascular disorders. *Blood*. 1998;91(10):3527–61.
 20. Yue KY, Zhang PR, Zheng MH, Cao XL, Cao Y, Zhang YZ, Zhang YF, Wu HN, Lu ZH, Liang L, Jiang XF, Han H. Neurons can upregulate Cav-1 to increase intake of endothelial cells-derived extracellular vesicles that attenuate apoptosis via miR-1290. *Cell Death Dis*. 2019;10(12):869. <https://doi.org/10.1038/s41419-019-2100-5>.
 21. Jansen F, Yang X, Hoelscher M, Cattelani A, Schmitz T, Proebsting S, Wenzel D, Vosen S, Franklin BS, Fleischmann BK, Nickenig G, Werner N. Endothelial microparticle-mediated transfer of MicroRNA-126 promotes vascular endothelial cell repair via SPRED1 and is abrogated in glucose-damaged endothelial microparticles. *Circulation*. 2013;128(18):2026–38. <https://doi.org/10.1161/CIRCULATIONAHA.113.001720>.
 22. Jansen F, Yang X, Hoyer FF, Paul K, Heiermann N, Becher MU, Abu HN, Kebschull M, Bedorf J, Franklin BS, Latz E, Nickenig G, Werner N. Endothelial microparticle uptake in target cells is annexin I/phosphatidylserine receptor dependent and prevents apoptosis. *Arterioscler Thromb Vasc Biol*. 2012;32(8):1925–35. <https://doi.org/10.1161/ATVBAHA.112.253229>.
 23. Chironi GN, Boulanger CM, Simon A, Dignat-George F, Freyssinet JM, Tedgui A. Endothelial microparticles in diseases. *Cell Tissue Res*. 2009;335(1):143–51. <https://doi.org/10.1007/s00441-008-0710-9>.
 24. Singh R, Barden A, Mori T, Beilin L. Advanced glycation end-products: a review. *Diabetologia*. 2001;44(2):129–46. <https://doi.org/10.1007/s001250051591>.
 25. Wautier JL, Schmidt AM. Protein glycation: a firm link to endothelial cell dysfunction. *Circ Res*. 2004;95(3):233–8. <https://doi.org/10.1161/01.RES.0000137876.28454.64>.
 26. Goldin A, Beckman JA, Schmidt AM, Creager MA. Advanced glycation end products: sparking the development of diabetic vascular injury.

- Circulation. 2006;114(6):597–605. <https://doi.org/10.1161/CIRCULATIONAHA.106.621854>.
27. Jing C, Zhang G, Liu Z, Xu Q, Li C, Cheng G, Shi R. Peroxidase promotes diabetic vascular endothelial dysfunction induced by advanced glycation end products via NOX2/HOCl/Akt/eNOS pathway. *Redox Biol.* 2021;45: 102031. <https://doi.org/10.1016/j.redox.2021.102031>.
 28. Xu F, Zhong JY, Lin X, Shan SK, Guo B, Zheng MH, Wang Y, Li F, Cui RR, Wu F, Zhou E, Liao XB, Liu YS, Yuan LQ. Melatonin alleviates vascular calcification and ageing through exosomal miR-204/miR-211 cluster in a paracrine manner. *J Pineal Res.* 2020;68(3): e12631. <https://doi.org/10.1111/jpi.12631>.
 29. Guay C, Kruit JK, Rome S, Menoud V, Mulder NL, Jurdzinski A, Mancarella F, Sebastiani G, Donda A, Gonzalez BJ, Jandus C, Bouzakri K, Pinget M, Boitard C, Romero P, Dotta F, Regazzi R. Lymphocyte-derived exosomal microRNAs promote pancreatic beta cell death and may contribute to type 1 diabetes development. *Cell Metab.* 2019;29(2):348–361.e6. <https://doi.org/10.1016/j.cmet.2018.09.011>.
 30. Catalano M, O'Driscoll L. Inhibiting extracellular vesicles formation and release: a review of EV inhibitors. *J Extracell Vesicles.* 2020;9(1):1703244. <https://doi.org/10.1080/20013078.2019.1703244>.
 31. Ding L, Yin Y, Hou Y, Jiang H, Zhang J, Dai Z, Zhang G. MicroRNA-214–3p suppresses ankylosing spondylitis fibroblast osteogenesis via BMP-TGFβ Axis and BMP2. *Front Endocrinol.* 2020;11:609753. <https://doi.org/10.3389/fendo.2020.609753>.
 32. Bartel DP. MicroRNAs. *Cell.* 2018;173(1):20–51. <https://doi.org/10.1016/j.cell.2018.03.006>.
 33. O'Brien K, Breyne K, Ughetto S, Laurent LC, Breakefield XO. RNA delivery by extracellular vesicles in mammalian cells and its applications. *Nat Rev Mol Cell Biol.* 2020;21(10):585–606. <https://doi.org/10.1038/s41580-020-0251-y>.
 34. Zhu J, Liu B, Wang Z, Wang D, Ni H, Zhang L, Wang Y. Exosomes from nicotine-stimulated macrophages accelerate atherosclerosis through miR-21–3p/PTEN-mediated VSMC migration and proliferation. *Theranostics.* 2019;9(23):6901–19. <https://doi.org/10.7150/thno.37357>.
 35. Kaur A, Mackin ST, Schlosser K, Wong FL, Elharram M, Delles C, Stewart DJ, Dayan N, Landry T, Pilote L. Systematic review of microRNA biomarkers in acute coronary syndrome and stable coronary artery disease. *Cardiovasc Res.* 2020;116(6):1113–24. <https://doi.org/10.1093/cvr/cvz302>.
 36. Zhang H, Wu J, Wu J, Fan Q, Zhou J, Wu J, Liu S, Zang J, Ye J, Xiao M, Tian T, Gao J. Exosome-mediated targeted delivery of miR-210 for angiogenic therapy after cerebral ischemia in mice. *J Nanobiotechnology.* 2019;17(1):29. <https://doi.org/10.1186/s12951-019-0461-7>.
 37. Singh N, Heggermont W, Fieuws S, Vanhaecke J, Van Cleemput J, De Geest B. Endothelium-enriched microRNAs as diagnostic biomarkers for cardiac allograft vasculopathy. *J Heart Lung Transplant.* 2015;34(11):1376–84. <https://doi.org/10.1016/j.healun.2015.06.008>.
 38. Chin DD, Poon C, Wang J, Joo J, Ong V, Jiang Z, Cheng K, Plotkin A, Magee GA, Chung EJ. miR-145 micelles mitigate atherosclerosis by modulating vascular smooth muscle cell phenotype. *Biomaterials.* 2021;273: 120810. <https://doi.org/10.1016/j.biomaterials.2021.120810>.
 39. Gomez I, Ward B, Souilhol C, Recarti C, Ariaans M, Johnston J, Burnett A, Mahmoud M, Luong LA, West L, Long M, Parry S, Woods R, Hulston C, Benedikter B, Niespolo C, Bazaz R, Francis S, Kiss-Toth E, van Zandvoort M, Schober A, Hellewell P, Evans PC, Ridger V. Neutrophil microvesicles drive atherosclerosis by delivering miR-155 to atheroprone endothelium. *Nat Commun.* 2020;11(1):214. <https://doi.org/10.1038/s41467-019-14043-y>.
 40. Lee KS, Hong SH, Bae SC. Both the Smad and p38 MAPK pathways play a crucial role in Runx2 expression following induction by transforming growth factor-beta and bone morphogenetic protein. *Oncogene.* 2002;21(47):7156–63. <https://doi.org/10.1038/sj.onc.1205937>.
 41. Wang S, Hu S, Wang J, Liu Y, Zhao R, Tong M, Cui H, Wu N, Chen X. Conditioned medium from bone marrow-derived mesenchymal stem cells inhibits vascular calcification through blockade of the BMP2-Smad1/5/8 signaling pathway. *Stem Cell Res Ther.* 2018;9(1):160. <https://doi.org/10.1186/s13287-018-0894-1>.
 42. Wang L, Li Y, Guo B, Zhang J, Zhu B, Li H, Ding Y, Meng B, Zhao H, Xiang L, Dong J, Liu M, Zhang J, Xiang L, Xiang G. Myeloid-derived growth factor promotes intestinal glucagon-like peptide-1 production in male mice with type 2 diabetes. *Endocrinology.* 2020. <https://doi.org/10.1210/endo/bqaa003>.
 43. Platko K, Lebeau PF, Guyalay G, Lhotak S, MacDonald ME, Pacher G, Hyun BJ, Boivin FJ, Igldoura SA, Cutz JC, Bridgewater D, Ingram AJ, Krepsinsky JC, Austin RC. TDAG51 (T-Cell Death-Associated Gene 51) is a key modulator of vascular calcification and osteogenic transdifferentiation of arterial smooth muscle cells. *Arterioscler Thromb Vasc Biol.* 2020;40(7):1664–79. <https://doi.org/10.1161/ATVBAHA.119.313779>.
 44. de Abreu RC, Fernandes H, Da CMP, Sahoo S, Emanuelli C, Ferreira L. Native and bioengineered extracellular vesicles for cardiovascular therapeutics. *Nat Rev Cardiol.* 2020;17(11):685–97. <https://doi.org/10.1038/s41569-020-0389-5>.
 45. Kalluri R, LeBleu VS. The biology, function, and biomedical applications of exosomes. *Science.* 2020. <https://doi.org/10.1126/science.aau6977>.
 46. Wiklander O, Brennan MA, Lotvall J, Breakefield XO, El AS. Advances in therapeutic applications of extracellular vesicles. *Sci Transl Med.* 2019. <https://doi.org/10.1126/scitranslmed.aav8521>.
 47. Yuan LQ. Novel strategies for gene therapy—recent advances in the use of exosomes for disease treatment. *Curr Pharm Des.* 2019;25(42):4463. <https://doi.org/10.2174/138161282542191230114518>.
 48. Liu C, Bayado N, He D, Li J, Chen H, Li L, Li J, Long X, Du T, Tang J, Dang Y, Fan Z, Wang L, Yang PC. Therapeutic Applications of Extracellular Vesicles for Myocardial Repair. *Front Cardiovasc Med.* 2021;8:758050. <https://doi.org/10.3389/fcvm.2021.758050>.
 49. Herrmann IK, Wood M, Fuhrmann G. Extracellular vesicles as a next-generation drug delivery platform. *Nat Nanotechnol.* 2021;16(7):748–59. <https://doi.org/10.1038/s41565-021-00931-2>.
 50. Wu P, Zhang B, Ocansey D, Xu W, Qian H. Extracellular vesicles: A bright star of nanomedicine. *Biomaterials.* 2021;269: 120467. <https://doi.org/10.1016/j.biomaterials.2020.120467>.
 51. Monaco F, Gaetani S, Alessandrini F, Tagliabracchi A, Bracci M, Valentino M, Neuzil J, Amati M, Bovenzi M, Tomasetti M, Santarelli L. Exosomal transfer of miR-126 promotes the anti-tumour response in malignant mesothelioma: Role of miR-126 in cancer-stroma communication. *Cancer Lett.* 2019;463:27–36. <https://doi.org/10.1016/j.canlet.2019.08.001>.
 52. Yu Y, Zhou H, Xiong Y, Liu J. Exosomal miR-199a-5p derived from endothelial cells attenuates apoptosis and inflammation in neural cells by inhibiting endoplasmic reticulum stress. *Brain Res.* 2020;1726: 146515. <https://doi.org/10.1016/j.brainres.2019.146515>.
 53. Jiang Y, Xie H, Tu W, Fang H, Ji C, Yan T, Huang H, Yu C, Hu Q, Gao Z, Lv S. Exosomes secreted by HUVECs attenuate hypoxia/reoxygenation-induced apoptosis in neural cells by suppressing miR-21–3p. *Am J Transl Res.* 2018;10(11):3529–41.
 54. Lin X, He Y, Hou X, Zhang Z, Wang R, Wu Q. Endothelial cells can regulate smooth muscle cells in contractile phenotype through the miR-206/ARF6/NCX1/Exosome Axis. *PLoS ONE.* 2016;11(3): e0152959. <https://doi.org/10.1371/journal.pone.0152959>.
 55. Nie C, Li Y, Qian H, Ying H, Wang L. Advanced glycation end products in food and their effects on intestinal tract. *Crit Rev Food Sci Nutr.* 2020. <https://doi.org/10.1080/10408398.2020.1863904>.
 56. McCance DR, Dyer DG, Dunn JA, Bailie KE, Thorpe SR, Baynes JW, Lyons TJ. Maillard reaction products and their relation to complications in insulin-dependent diabetes mellitus. *J Clin Invest.* 1993;91(6):2470–8. <https://doi.org/10.1172/JCI116482>.
 57. Hudson BI, Lippman ME. Targeting RAGE Signaling in Inflammatory Disease. *Annu Rev Med.* 2018;69:349–64. <https://doi.org/10.1146/annurev-med-041316-085215>.
 58. Sharma A, Weber D, Raupbach J, Dakal TC, Fliesbach K, Ramirez A, Grune T, Wullner U. Advanced glycation end products and protein carbonyl levels in plasma reveal sex-specific differences in Parkinson's and Alzheimer's disease. *Redox Biol.* 2020;34: 101546. <https://doi.org/10.1016/j.redox.2020.101546>.
 59. Zeng P, Yang J, Liu L, Yang X, Yao Z, Ma C, Zhu H, Su J, Zhao Q, Feng K, Yang S, Zhu Y, Li X, Wang W, Duan Y, Han J, Chen Y. ERK1/2 inhibition reduces vascular calcification by activating miR-126–3p-DKK1/LRP6 pathway. *Theranostics.* 2021;11(3):1129–46. <https://doi.org/10.7150/thno.49771>.
 60. Tang L. Recapitulating miRNA biogenesis in cells. *Nat Methods.* 2022;19(1):35. <https://doi.org/10.1038/s41592-021-01385-z>.
 61. Goodall GJ, Wickramasinghe VO. RNA in cancer. *Nat Rev Cancer.* 2021;21(1):22–36. <https://doi.org/10.1038/s41568-020-00306-0>.
 62. Treiber T, Treiber N, Meister G. Regulation of microRNA biogenesis and its crosstalk with other cellular pathways. *Nat Rev Mol Cell Biol.* 2019;20(1):5–20. <https://doi.org/10.1038/s41580-018-0059-1>.
 63. Guo FH, Guan YN, Guo JJ, Zhang LJ, Qiu JJ, Ji Y, Chen AF, Jing Q. Single-Cell Transcriptome Analysis Reveals Embryonic Endothelial Heterogeneity at Spatiotemporal Level and Multifunctions of MicroRNA-126 in Mice. *Arterioscler Thromb Vasc Biol.* 2022;42(3):326–42. <https://doi.org/10.1161/ATVBAHA.121.317093>.

64. Wu M, Chen G, Li YP. TGF-beta and BMP signaling in osteoblast, skeletal development, and bone formation, homeostasis and disease. *Bone Res.* 2016;4:16009. <https://doi.org/10.1038/boneres.2016.9>.
65. Afzal F, Pratap J, Ito K, Ito Y, Stein JL, van Wijnen AJ, Stein GS, Lian JB, Javed A. Smad function and intranuclear targeting share a Runx2 motif required for osteogenic lineage induction and BMP2 responsive transcription. *J Cell Physiol.* 2005;204(1):63–72. <https://doi.org/10.1002/jcp.20258>.
66. Franceschi RT, Xiao G. Regulation of the osteoblast-specific transcription factor, Runx2: responsiveness to multiple signal transduction pathways. *J Cell Biochem.* 2003;88(3):446–54. <https://doi.org/10.1002/jcb.10369>.

Publisher's Note

Springer Nature remains neutral with regard to jurisdictional claims in published maps and institutional affiliations.

Ready to submit your research? Choose BMC and benefit from:

- fast, convenient online submission
- thorough peer review by experienced researchers in your field
- rapid publication on acceptance
- support for research data, including large and complex data types
- gold Open Access which fosters wider collaboration and increased citations
- maximum visibility for your research: over 100M website views per year

At BMC, research is always in progress.

Learn more biomedcentral.com/submissions

